Resonances of a coated sphere

T. M. Bambino
Centro Brasileiro de Pesquisas Físicas, Rua Xavier Sigaud 150, Rio de Janeiro 22.290, Brazil

L. G. Guimarães
Departamento de Física Nuclear, Instituto de Física, Universidade Federal do Rio de Janeiro, Caixa Postal 68528, 21945-970, Rio de Janeiro, Brazil

(Received 24 May 1995)

In the scattering of a plane wave by a perfectly conducting sphere coated with a dieletric layer, we show that the layer thickness plays an important role in the resonance position and the cross section profile. To do this, we developed a method to calculate the resonance position and width. A physical interpretation of these resonant modes is given based on the analogy between optics and quantum mechanics.

PACS number(s): 42.25.Bs, 42.25.Fx, 42.25.Gy, 42.68.Mj

I. INTRODUCTION

In recent years light scattering by micrometer sized particles has been a subject of research in a wide range of fields. For instance, on light scattering by micrometer droplets many quantum optical effects, such as stimulated Raman and Brillouin scattering and lasing, were observed [1–3]. These nonlinear optical processes occur in regions where the electromagnetic field strength is high. In Mie scattering the light is scattered by a dielectric sphere [4]. In resonant conditions the field is strong in regions near and inside the spherical surface [5,6]. Those experimental results show that micrometer dielectric spheres can be good optical resonant cavities. An interesting variation of the Mie scattering is the Aden and Kerker scattering (AK). In AK scattering an incident plane wave with vector wave k is scattered by a dielectric spherical core coated with a dielectric spherical layer [7,8]. In the present work, we will study the AK scattering in the particular situation in which the light is scattered by a perfectly metallic core coated with a transparent layer [9–12] with real vacuum relative refractive index $N > 1$. As in Mie scattering, as well as in AK scattering, the electromagnetic fields are given by infinite partial wave expansion [7,8]. The AK scattering resonant modes are related to the complex poles of this partial wave expansion. These poles are the solutions of the following transcendental equation:

$$N\epsilon_j F_\ell^j(\alpha,\gamma) = V_\ell^j(\alpha,\gamma)\ln'[\zeta_\ell^{(1)}(\beta)]. \tag{1.1}$$

Here $\ln'(\zeta_\ell^{(1)})$ denotes the Ricatti-Hankel function logarithmic derivative with respect to the argument. The index j is the polarization index so that the symbol ϵ_j assumes the values $\epsilon_1 = 1$ ($j = 1$ perpendicular polarization or magnetic waves M) and $\epsilon_2 = 1/N^2$ ($j = 2$ parallel polarization or electric waves E). We define the size parameters $\beta = kb$ (b being the outer radius), $\alpha = N\beta$, and $\gamma = Nka$ ($b = \rho a$, a being the core radius). Besides, for the ℓth resonant multipole the functions F_ℓ^j and V_ℓ^j are written as

$$F_\ell^j(\alpha,\gamma) \equiv \begin{cases} \psi_\ell'(\alpha)\chi_\ell(\gamma) - \chi_\ell'(\alpha)\psi_\ell(\gamma), & j = 1 \\ \psi_\ell'(\alpha)\chi_\ell'(\gamma) - \chi_\ell'(\alpha)\psi_\ell'(\gamma), & j = 2, \end{cases} \tag{1.2}$$

$$V_\ell^j(\alpha,\gamma) \equiv \begin{cases} \psi_\ell(\alpha)\chi_\ell(\gamma) - \chi_\ell(\alpha)\psi_\ell(\gamma), & j = 1 \\ \psi_\ell(\alpha)\chi_\ell'(\gamma) - \chi_\ell(\alpha)\psi_\ell'(\gamma), & j = 2, \end{cases} \tag{1.3}$$

where ψ and χ are the Ricatti-Bessel and the Ricatti-Neumann functions, respectively. The solutions of Eq. (1.1) for a given multipole ℓ are complex and can be written in the form, $\overline{\beta} = \beta - iw$, where β and w are the resonance position and resonance width, respectively.

II. PHYSICAL INTERPRETATION OF AK RESONANCES

In the case of the micrometer coated spheres, optical resonances are related to high ℓ values, so that these resonance calculations need suitable numerical computational efforts [13–16]. The physical interpretation of these resonances can be understood with the help of the well-known analogy of optics and quantum mechanical scattering. It is well known that the Hertz-Debye electromagnetic scalar potentials [4,8] can be interpreted as solutions of a Schrödinger-like equation subject to an effective potential U_{eff} [6,17–19]. In the present case, for the ℓth partial wave and an incident "particle" having energy k^2, the effective potential U_{eff} (in units such that $\hbar = 2m = 1$) takes the form of an attractive square well of depth $k^2(N^2 - 1)$ (see Fig. 1) plus the centrifugal potential (λ^2/r^2) with $\lambda = \ell + 1/2$ (Langer semiclassical modification) representing the angular momentum. In this approach, resonances can be interpreted as quasibound states of the light [6,17–19]. In the geometrical optics approximation the strong fields can occur in regions delimited by two concentric aplanatic spheres $r = b/N$ and $r = Nb$ [6,20], so that in resonance studies the ratio $b/(aN)$ plays an important role. For instance, if the core radius a is less than the internal aplanatic sphere radius b/N, the AK scattering becomes very similar to Mie scat-

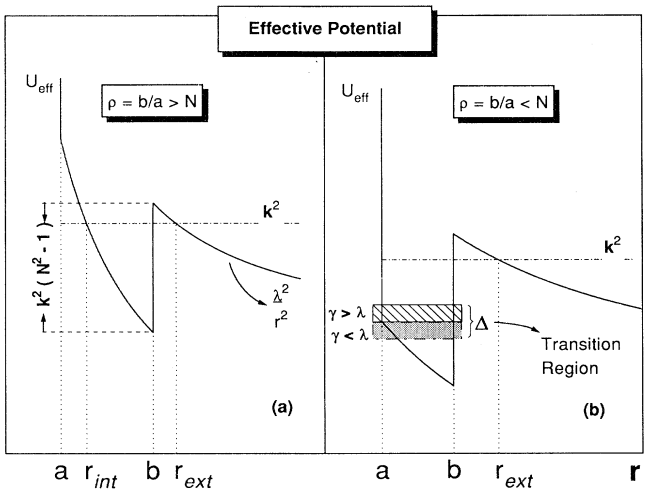

FIG. 1. Effective potential U_{eff} for a spherical metallic core of radius a coated by a transparent spherical dielectric layer of radius b and having the vacuum relative refractive index $N > 1$. Within this framework, resonances are interpreted as quasibound states of the light. In (a) as the $b/a > N$, the metallic core volume is smaller than the layer volume so that the AK resonances are very similar to Mie resonances. On the other hand, in (b) as the $b/a < N$, reflections on the metallic core surface are not negligible and the Δ region characterizes the transition between the Mie-like resonances ($\gamma < \lambda$) to the Fabry-Pérot-like ($\gamma > \lambda$) AK resonances.

tering, so that the AK resonant spectrum behaves like the resonant Mie spectrum [see Fig. 1(a)] and the size parameters satisfy the inequality $\gamma < \beta < \lambda < \alpha$. Otherwise, if $a > b/N$ there are two different possibilities to be analyzed. The first situation occurs for impact parameters such that reflections on metallic core surface start becoming important. This situation is related to size parameters that satisfy the inequality $\beta < \gamma < \lambda < \alpha$. In the other situation, when $\beta < \lambda < \gamma < \alpha$ the layer thickness is very thin, so that the resonant modes can be interpreted as surface waves that travel around a thin dielectric spherical layer. In this case the AK scattering resembles the scattering by a thin film [16,21] and the resonances are qualitatively equivalent to Fabry-Pérot cavity normal modes [see Fig. 1(b)]. In the case $a > bN$ and a given λ, we denote the transition region Δ [see Fig. 1(b)] as being the resonances for which $|\gamma - \lambda| \sim O(\lambda^{1/3})$. This region is very singular. For resonances in the Δ transition region, the boundary conditions at the spherical metallic core play a central role, as we will see soon.

III. ASYMPTOTIC FORMULAS TO AK RESONANCES

For Mie-like and Fabry-Pérot-like resonances, we can apply the semiclassical Bohr-Sommerfeld quantization rule. In this approximation the resonance positions are polarization independent and are determined by

$$\int_{r_0}^{b} dr \sqrt{N^2 k_{nj}^2 - (\lambda/r)^2} = (n + 1/2)\pi;$$

$$n = 0, 1, ...n_{\max} - 1, \quad (3.1)$$

where the integer n is the resonance order and $n_{\max}$ is the maximum number of allowed resonances inside the effective well. The turning point r_0 assumes the values $r_0 = r_{int} = \lambda/(Nk)$ in the case of Mie-like resonances ($\gamma < \lambda$) and $r_0 = a$ for Fabry-Pérot-like resonances ($\gamma > \lambda$) [see Figs. 1(a) and (b)]. For a given λ and ρ, the resonance positions are labeled by polarization j and order n as $\beta \to \beta_{nj}(\lambda, \rho)$, or in a more compact notation by the symbol $j_n^{\lambda - 1/2}$. In this semiclassical approximation the resonance width w_{nj} is proportional to the barrier penetration factor,

$$w_{nj} \propto \exp\left[-2 \int_b^{r_{ext}} dr \sqrt{(\lambda/r)^2 - k_{nj}^2}\right]. \quad (3.2)$$

The external turning point is $r_{ext} = \lambda/k$ [see Figs. 1(a) and (b)]. Equation (3.2) shows that for high λ angular momentum values, the resonances can be extremely sharp. For resonances values in the Δ transition region ($\gamma \sim \lambda$) the Bohr-Sommerfeld quantization rule does not hold. In this case, we need to develop another approximation method to calculate the AK resonances. The *localization principle* [4,6] relates the resonances to an incident ray that tunnels through the barrier. These particular rays have angular momentum λ greater than the resonance position β. Applying this fact and the sharp resonance limit to Eq. (1.1), we can obtain more suitable formulas to the resonance position β and width w, namely,

$$\beta_{nj}[\mathrm{AK}] \approx \beta_{nj}[\mathrm{Mie}] + \Delta\beta_{nj}[Mie] + O(\lambda^{-2/3}), \quad (3.3)$$

$$w_{nj} \approx \left\{ \frac{[\frac{\lambda^2}{\beta^2} - 1]}{\ln' \chi_\ell(\beta)} - \ln' \chi_\ell(\beta) - N[S_\ell^j(\alpha) + \frac{S_\ell^j(\gamma)}{\rho}] \right\}^{-1} Y_\ell, \quad (3.4)$$

where $Y_\ell \equiv [\chi_\ell(\beta)\chi'_\ell(\beta)]^{-1}$ and

$$S_\ell^j(x) \equiv (F_\ell^j)^{-1} \frac{\partial F_\ell^j}{\partial x} - (V_\ell^j)^{-1} \frac{\partial V_\ell^j}{\partial x} F_\ell^j. \quad (3.5)$$

The right-hand side of Eq. (3.3) is calculated at Mie resonance values. This equation allows us to approximate any AK resonance by an equivalent Mie resonance plus a remainder term $\Delta\beta$. In this approximation this remainder term is written as

$$\Delta\beta \equiv -T_\ell^j \left\{ N(1 - \epsilon_j)\psi'_\ell(\alpha)^2 + \frac{[\lambda\psi_\ell(\alpha)]^2}{N\beta^2} c_j + \psi_\ell(\alpha)^2 d_j \right\}^{-1}. \quad (3.6)$$

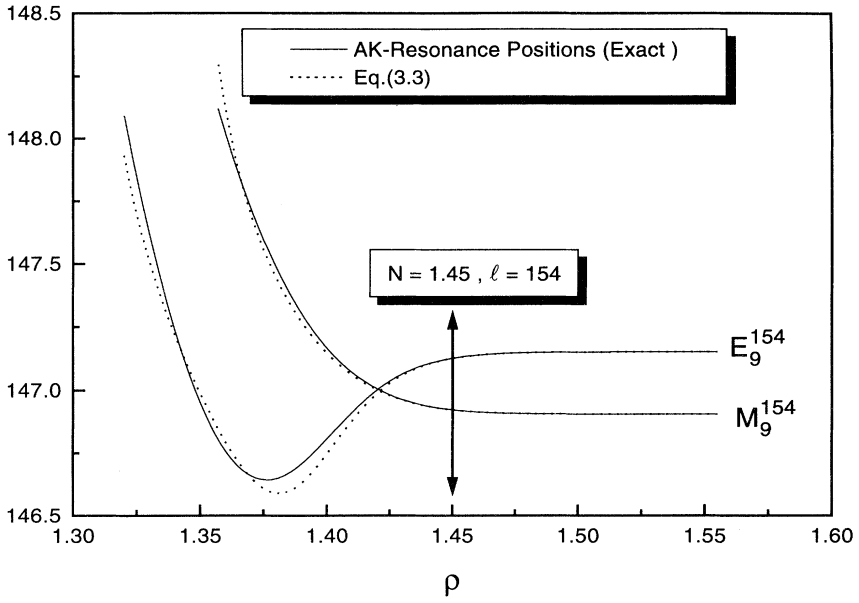

FIG. 2. AK resonance positions (for E and M polarization) as the layer thickness varies, for $N = 1.45$ (silica) and resonant multipole $\ell = 154$. The full line is the exact numerical calculation obtained solving Eq. (1.1) and the dashed line is the result of applying Eq. (3.3). Note that the accuracy of Eq. (3.3) decreases for $\rho \leq N$. In this region, the resonances are in the Δ transition region and some interesting resonance behaviors begin to appear. For instance, the resonances E and M present a crossover position and the resonance related to E polarization has a minimum value.

Here, $c_j \equiv (\epsilon_j^{-1} - 1)$, $d_j \equiv N - (N\epsilon_j)^{-1}$, and the function T_ℓ^j assumes the values $T_\ell^1 \equiv \psi_\ell(\gamma)/\chi_\ell(\gamma)$ and $T_\ell^2 \equiv -\psi_\ell'(\gamma)/\chi_\ell'(\gamma)$. The advantage of applying Eq. (3.3) to calculate the AK resonance is to reduce it to the Mie resonance calculation. On the other hand, Mie resonance calculations need accuracy greater than their width. To supply this numerical requirement we use an algorithm that is based on uniform asymptotic expansion to Bessel functions [19], so that we can apply Eq. (3.3) for any ρ value as an initial guess to Eq. (1.1) in some exact numerical AK resonance calculation method. The accuracy of Eq. (3.3) is shown in Fig. 2 for two AK resonances.

IV. RESULTS AND AK RESONANCES SPECIAL FEATURES

Using the above numerical procedure we calculated for $N = 1.33$ the transition from all the Mie-like resonances ($\gamma \ll \lambda$) in the range $58.2 \leq \beta \leq 59$ to the Fabry-Pérot-like resonances ($\gamma \approx \lambda$). These results are shown in Fig. 3. It is interesting to observe the peculiar behavior of the AK resonances as compared to Mie resonances. In this context, Mie resonances are the asymptotic limit $\rho \gg N$ of the AK resonances. Figures 2 and 3 show that the relative separations between the AK resonances are strongly

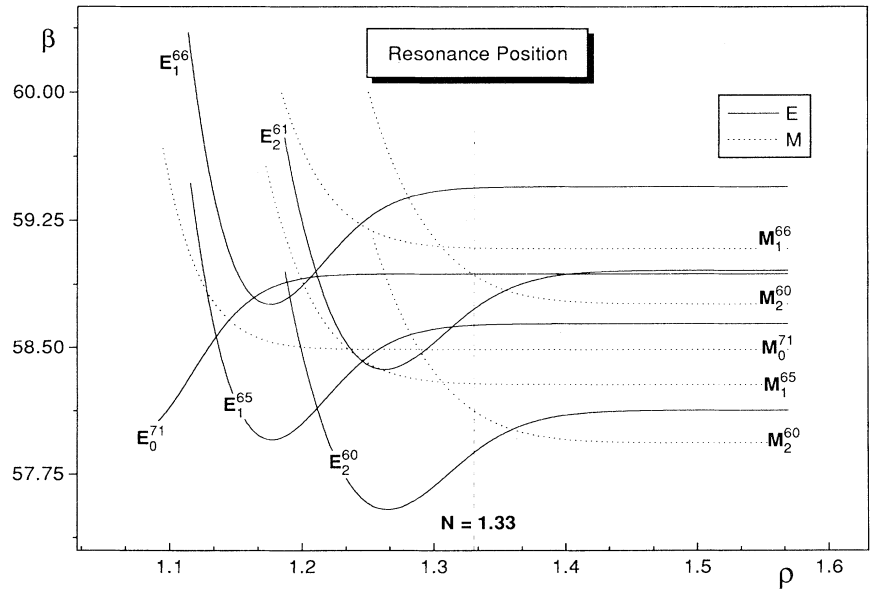

FIG. 3. AK resonance positions for $N = 1.33$ (water) (for E and M polarization) as ρ varies. Observe the transition from the all Mie like resonances ($\gamma \ll \lambda$) in the range $58.2 \leq \beta \leq 59$ to the Fabry-Pérot-like resonances ($\gamma \approx \lambda$). Notice that for ρ close to N (see vertical dashed and dotted line $\rho = 1.33$) some resonances present a crossover position and the resonances related to E polarization has a minimum value, which occurs for layer thicknesses in which γ is close to λ; more precisely, $\gamma \approx \lambda + O(\lambda^{-1/3})$.

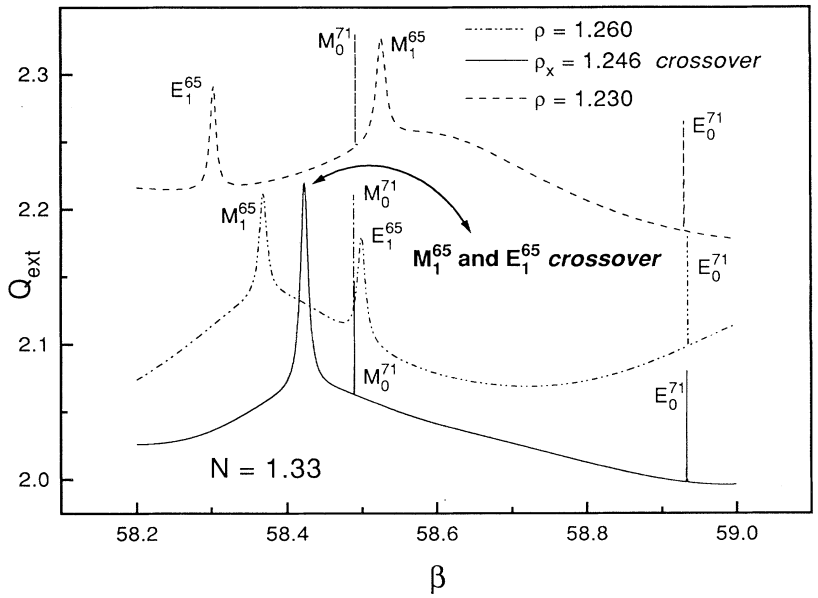

FIG. 4. Extinction efficiency factor Q_{ext} for $N = 1.33$ (water) as a function of the size parameter β in the case of the three different layer thicknesses. Note that for $\rho = \rho_x$ the resonances M_1^{65} and E_1^{65} have a crossover position. In this situation, their related peaks on the Q_{ext} curve are superimposed. Observe that slow ρ variations imply significant changes in the Q_{ext} curve.

modified as ρ varies. More precisely, we can observe the following particular features of the AK resonances. It is interesting to note that several resonances have a *crossover position* and the resonances related to E polarization have a *minimum value* as the layer thickness decreases. For resonances where the width values are similar, the resonance crossovers have great importance in the scattering features. On the other hand, the AK resonant spectrum is very similar to the *strong polarized electronic diatomic molecular spectrum* [22,23]. It is not a coincidence, but it is related to the similarity between the electromagnetic wave equation and Schrödinger equation. In both wave equations, tunneling and boundary conditions play a fundamental role in the spectrum behavior. In other words, the resonant E multipoles behave as *bonding molecular orbitals* and the resonant M multipoles as *antibonding molecular orbitals.* In the case of a dielectric core with refractive index N_{core} having a real part $\mathrm{Re}\{N_{core}\}$ greater than the layer refractive index N, the effective potential U_{eff} is a double well potential that resembles a model of polarized diatomic molecular potential [22,23]. For strong core absorption ($\mathrm{Im}\{N_{core}\} \gg 1$), the two wells do not have correlation. In this limit U_{eff} is equivalent to strong polarized diatomic molecular potential. Applying Debye and Schöbe asymptotic formulas to cylindrical Bessel functions [24], we obtained approximate formulas to crossover point ρ_x and minimum E-resonance point ρ_{min}. For resonances related to a given λ and n these formulas are, respectively,

$$\rho_x \sim N/M\Big[\tan^{-1}(M) + (n + 5/12)(\pi/\lambda) + p(0.795/\lambda)\Big]\left(1 + p/\lambda^{2/3}\right)^{-1}, \quad (4.1)$$

$$\rho_{min} \sim N/M\Big[tg^{-1}(M) + (n + 1/12)(\pi/\lambda) + N(0.918)/(M\lambda^{1/3})\Big], \quad (4.2)$$

where $M \equiv \sqrt{N^2 - 1}$ and $p \equiv 0.422 - \sqrt{0.178 + 1.11M}$. These size effects change the scattering efficiency factors [25,26]. Figure 4 shows the extinction efficiency factor $Q_{ext}(\beta)$ for some layer thickness values. In the size parameter β-plane, the sharp peaks that appear in the $Q_{ext}(\beta)$ figure are centered at some resonance value [17]. In the case of Fig. 4, the crossover between the resonances E_1^{65} and M_1^{65} can be seen as the superposition of two resonance peaks. Notice that the slow ρ variation makes significant changes in the Q_{ext} curve, so that resonant and nonresonant contributions to Q_{ext} are very sensitive to ρ variation.

V. CONCLUSIONS

Now we summarize some possible applications of the present work's results. For the case of the liquid droplet layer, we can apply the AK resonances calculations [Eq. (3.3)] to study the evaporation effects [see Figs. 2 and 3] in high precision particle size and geometry characterization experiments [25]. The resonant Mie scattering has been applied for the generation of several nonlinear optics [1–3] and cavity QED in visible [27] experiments. For experimental observation of these effects, we think that resonant AK scattering is more efficient than the resonant Mie scattering. This conclusion is based on the fact that in the resonant AK scattering, the near and internal light intensity can be greater than in the equivalent Mie scattering situation. More precisely, during AK resonances crossover [Eq. (4.1)], the internal and near electromagnetic field strength is at least twice that of the equivalent E or M polarization resonant Mie electromagnetic field strength. Besides, the AK resonance for E polarization at point of minimum ρ_{min} [Eq. (4.2)] is sharper than an equivalent Mie resonance. On the other hand, the internal maximum resonant field intensity values are related to the inverse resonance width [6]. Then for E

polarization and the layer thickness equal to $(\rho_{\min} - 1)a$, the resonant a AK scattering provides stronger fields than an equivalent Mie scattering. To finalize, based on the similarity between AK resonant spectrum and an electronic diatomic molecular spectrum (see Figs. 2 and 3), we think that in analogy with photonic band gap theory [28], a multilayered dielectric sphere can behave as a disordered optical system. For a large number of the layers, the optical effective potential becomes very similar to the electronic effective semiconductor potential. This multilayered system should exhibit strong photon localization [29] . Work on these issues is in progress, and we plan to present it in the near future.

ACKNOWLEDGMENTS

This work is supported in part by the Brazilian agencies CNPq and FINEP. We thank Professor Mauricio Ortiz Calvão and Professor Anibal Omar Caride for suggestions and many helpful discussions.

[1] P. G. Pinnick *et al.*, Opt. Lett. **13**, 494 (1988).
[2] I. Zhang and R. K. Chang, J. Opt. Soc. Am. B **6**, 151 (1989).
[3] S. X. Qian *et al.*, Science **231**, 486 (1986).
[4] H. C. van de Hulst, *Light Scattering by Small Particles* (Wiley, New York, 1957).
[5] V. Srivastava and M. A. Jarzimbsky, Opt. Lett. **16**, 126 (1991).
[6] L. G. Guimarães, Opt. Commun. **103**, 339 (1993).
[7] A. L. Aden and M. Kerker, J. Appl. Phys. **22**, 1242 (1951).
[8] M. Kerker, *The Scattering of Light and Other Electromagnetic Radiations* (Academic, New York, 1969).
[9] H. Scharfman, J. Appl. Phys. **25**, 1352 (1954).
[10] J. Rheinstein, IEEE Trans. Anten. Propag. **AP-12** , 334 (1964).
[11] E. L. Murphy, J. Appl. Phys. **36**, 1918 (1965).
[12] V. H. Weston and R. Hemenger, J. Res. Natl. Bur. Stand. Sec. D **66**, 613 (1962).
[13] A. B. Pluchino, Appl. Opt. **20**, 2986 (1981).
[14] R. L. Hightower and C. B. Richardson, Appl. Opt. **27**, 4850 (1988).
[15] T. Kaizer and G. Schweiger, Comput. Phys. **7**, 682 (1993).
[16] J. A. Lock, Appl. Opt. **29**, 3180 (1990).
[17] L. G. Guimarães and H. M. Nussenzveig, Opt. Commun. **89**, 363 (1992).
[18] B. R. Johnson, J. Opt. Soc. Am. A **10**, 343 (1993).
[19] L. G. Guimarães and H. M. Nussenzveig, J. Mod. Opt. **41**, 625 (1994).
[20] *Principles of Optics*, edited by M. Born and E. Wolf, (Pergamon, Oxford, 1970).
[21] C. F. Bohren, Appl. Opt. **27**, 205 (1988).
[22] J. C. Slater, *Quantum Theory of Molecules and Solids* (McGraw-Hill, New York, 1963).
[23] M. A. Morrison, T. L. Estle, and N. F. Lane, *Quantum States of Atoms, Molecules and Solids* (Prentice-Hall, Englewood Cliffs, NJ, 1976).
[24] *Handbook of Mathematical Functions*, edited by M. Abramowitz and I. Stegun (Dover, New York, 1965).
[25] R. L. Hightower *et al.*, Opt. Lett. **13**, 946 (1988).
[26] J. A. Lock, J. M. Jamison, and C. Y. Lin, Appl. Opt. **33**, 4677 (1994).
[27] A. J. Campillo, J. D. Eversole, and H. B. Lin, Phys. Rev. Lett. **67**, 437 (1991).
[28] E. Yablonovitch, Phys. Rev. Lett. **58**, 2059 (1987).
[29] S. John, Phys. Rev. Lett. **58**, 2486 (1987).